

## Solitary Waves as Fixed Points of Infinite-Dimensional Maps in an Optical Bistable Ring Cavity

D. W. Mc Laughlin, J. V. Moloney, and A. C. Newell

*Applied Mathematics and Optical Sciences Center, University of Arizona, Tucson, Arizona 85721*

(Received 13 April 1983)

Phase-locked solitary waves are shown to be the stable fixed points of an infinite-dimensional map obtained from a bistable optical ring cavity.

PACS numbers: 02.50.+s, 05.40.+j, 42.65.-k

The ultimate goal of these studies is to find methods for analyzing nonlinear systems which exhibit coherent spatial structure and temporal chaos and give every indication of lying on low-dimensional chaotic attractors. Efforts to date have followed the prescription of projecting the field variable into some finite-dimensional Galerkin basis thereby obtaining a finite set of nonlinear ordinary differential equations. These equations are then analyzed by direct integration or by converting the continuous time variable into appropriate discrete steps and obtaining a corresponding iterative map.<sup>1</sup> The trouble with the approach is that the truncation associated with the projection is rarely justified and the outcome is often sensitive to the dimension of the basis chosen to approximate the field variable. A key step, therefore, in the analysis of these situations is to find an appropriate basis in which the original infinite-dimensional system is almost separable and in which a few modes can capture its essential low-dimensional character. Solitary waves and solitons, although traditionally associated with integrable systems and not with the kind of chaotic dynamics often encountered in maps, are prime candidates for such a basis. Certainly this is a reasonable hope when the physics in question can be essentially modeled by an integrable system under external influences. One would then expect there to be certain parallels to the breakup of Kolmogorov-Arnold-Moser surfaces and homoclinic orbits in finite-dimensional systems such as the driven damped pendulum.<sup>2</sup>

In this Letter we make a start in the right direction by showing that solitary waves can be the fixed points of infinite-dimensional maps. In particular, our approach allows us to explain the spatial rings found by Moloney and Gibbs<sup>3</sup> in their numerical model of a bistable optical ring cavity. We anticipate that in wider parameter ranges we will find that these rings exhibit temporal chaos while yet maintaining a spatially co-

herent structure.

Consider Fig. 1(a). A unidirectional polarized input laser beam, propagating in the  $z$  direction, with an input profile which is Gaussian in one transverse direction, enters a nonlinear medium at point  $H$ ,  $z = 0$  at  $t = 0$ . After propagating through the medium to point  $I$ ,  $z = L_1$ , the beam is then reflected through four mirrors (two of which reduce its intensity) so as to re-enter the nonlinear medium at time  $t_0 = (L_1 + L_2)/c$ , and reinforce the original pump field. The signal continues to circulate around the cavity and our goal is to predict the output after many passes.

The input laser beam signal is  $\vec{E}_{in}(x, z, t) = 2 \operatorname{Re}\{A(x) \exp[i(kz - \omega t)]\} \hat{r}$ ,  $k = \omega/c$ , where  $A(x)$  has a prescribed shape. In the nonlinear medium

$$\vec{E}(x, z, t) = 2 \operatorname{Re}\{B(x, z, t) \exp[i(kz - \omega t)]\} \hat{r}, \quad (1)$$

where the envelope  $B$  satisfies

$$\frac{\partial B}{\partial z} + \frac{1}{c} \frac{\partial B}{\partial t} = -\frac{\alpha_0}{2} \left[ \frac{1 + i\Delta}{1 + \Delta^2 + BB^*} - \frac{i \ln 2}{4\pi \alpha_0 L_1 F} \frac{\partial^2}{\partial x^2} \right] B. \quad (2)$$

Here  $\alpha_0$  is the linear absorption per unit length,  $\Delta$  is the laser-atom detuning normalized to the dipole decay width, and  $F$ , which we assume to be large, is the Fresnel number measuring the transverse diffraction of the beam. To describe the evolution of the field through the nonlinear medium by Eq. (2), we have assumed (see Ref. 3 for details) that (a) the nonlinear medium inversion and dipole relaxation times are short compared to the cavity roundtrip time  $t_0$  and that (b) there is no significant steepening in the propagation direction. In the linear return medium  $IJKH$ , we simply assume that the field satisfies the linear wave equation,

$$\vec{E}(x, z = L, t) = \vec{E}(x, z = L_1, t - L_2/c), \quad L = L_1 + L_2.$$

The infinite-dimensional map is obtained as follows. Consider the field  $\vec{E}(x, 0, t)$  at  $z = 0$  in the various time intervals  $I_n$ ,  $(n-1)t_0 < t < nt_0$ .

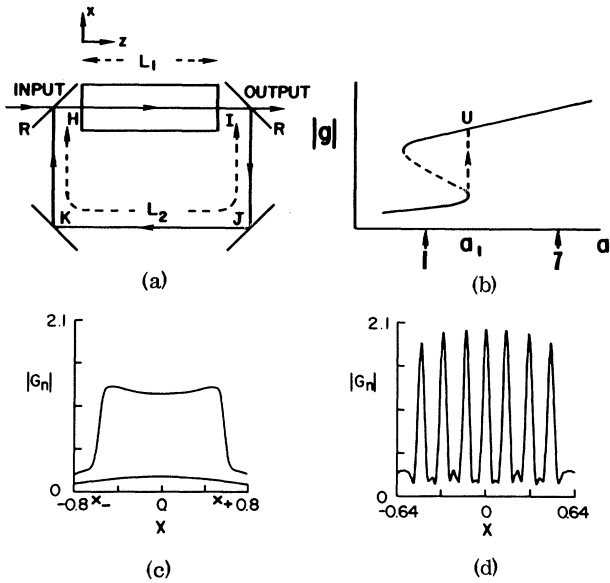


FIG. 1. (a) Unidirectional passive ring cavity containing a nonlinear (two-level atom) saturable medium of length  $L_1$ . (b) Schematic of the plane-wave bistable loop obtained from the steady-state solution (fixed point) of Eq. (7), for  $R=0.9$ ,  $p=2$ , and  $kL=0.4$  rad. When transverse effects are included [solve Eq. (5) with boundary condition (6) and  $F=200$ ] stationary  $N$ -solitary-wave trains appear on the high-transmission branch at equal increments of  $a(0)$ , the peak input Gaussian field amplitude ( $N=1, 7$  are indicated by upward arrows). The same parameter values are used to generate all subsequent results. (c) Initiation of the seven-solitary-wave train from the sharp gradients on the outer edges of the transverse laser beam (intracavity field on the 23rd pass). The final steady-state transverse pulses are confined to the interval  $(x_+, x_-) = (0.61, -0.61)$ . The lower trace in this figure shows the much broader Gaussian profile after propagating through the nonlinear medium once. (d) Steady-state seven-solitary-wave train at  $a(0) = 0.194$  evolving from the transient in (c) after 200 cavity passes.

For  $0 < t < t_0$ ,  $\vec{E}(x, 0, t) = 2 \text{Re}[\sqrt{TA}(x)e^{-i\omega t}] \hat{r}$ . For  $t_0 < t < 2t_0$ ,  $\vec{E}(x, 0, t) = 2 \text{Re}[\sqrt{TA}(x)e^{-i\omega t}] \hat{r} + R\vec{E}(x, L_1, t - L_2/c)$ . Here  $R$  is the reflection coefficient at the mirrors at  $H, I$  (a large fraction  $R$  of the intensity is reflected) and  $T$  the transmission coefficient. Observe that  $B$  is a function of  $t$  only through  $\tau = t - z/c$  and Eq. (2) tells us how  $B$  evolves as a function of  $z$  for fixed  $\tau$ . The dependence of  $B$  on  $\tau$  is determined by the data at  $z = 0$ . But  $A(x)$  is independent of  $t$  and therefore, on the first pass,  $B$  is. Similarly in the  $n$ th interval  $I_n$ , the envelope of  $e^{-i\omega t}$  at  $z = 0$  is independent of  $t$ . Therefore we can simply replace

the dependence of  $B$  on  $t$  by stating in which interval it has been generated. On the  $n$ th pass the initial condition at  $z = 0$  is

$$\vec{E}(x, 0, t) = 2\hat{r} \text{Re}[\sqrt{TA}(x) + RB_{n-1}(x, z=L_1)e^{ikL}]e^{-i\omega t}$$

and so we can write

$$B_n(x, z=0) = \sqrt{TA}(x) + RB_{n-1}(x, z=L_1)e^{ikL}, \quad (3)$$

$B_0 = 0$ . Our task is to determine the limit of  $B_n(x, z=0)$  as  $n \rightarrow \infty$  if it exists. It is useful to introduce the new variables

$$p = \frac{\alpha L_1}{\Delta}, \quad f = \frac{4\pi F}{\ln 2 p}, \quad \xi = \frac{\alpha}{\Delta} z, \quad y = \sqrt{f} x,$$

$$a(y) = \left(\frac{T}{2\Delta^2}\right)^{1/2} A\left(\frac{y}{\sqrt{f}}\right), \quad (4)$$

$$G_n(y, \xi) = \frac{1}{\sqrt{2\Delta}} B_n\left(\frac{y}{\sqrt{f}}, L_1 \frac{\xi}{p}\right)$$

whence (2) and (3) become

$$2i \frac{\partial G_n}{\partial \xi} + \frac{\partial^2 G_n}{\partial y^2} - \frac{G_n}{1 + 2G_n G_n^*} = 0, \quad (5)$$

$$G_n(y, 0) = a(y) + \text{Re}^{ikL} G_{n-1}(y, p), \quad (6)$$

$n > 1$ ,  $G_0 = 0$ . In (5), we have omitted the attenuation and other terms of order  $1/\Delta$  as they are assumed to be small. Equation (6), which acts as the initial data for the solution of (5) during the  $n$ th pass through the nonlinear medium, is the infinite-dimensional map of interest.

In order to understand the dynamics in the case when  $f \gg 1$  and the input transverse profile is Gaussian-like, it is first necessary to understand what happens when  $a(y)$  and therefore  $G$  are independent of the transverse coordinate. This is called the plane-wave case. Then the solution of (5) is trivial and one finds

$$G_n(y, p) = G_n(y, 0) \exp[-i(p/2)g(|G_n(y, 0)|)],$$

where  $g(|G|) = (1 + 2|G|^2)^{-1}$ . In this case (6) is a one-dimensional complex map from one member of the sequence  $[G_n(y, 0) = g_n]_{n=0}$  to the next:

$$g_{n+1} = a + Rg_n \exp[ikL - i(p/2)(1 + 2|g_n|^2)^{-1}]. \quad (7)$$

Its fixed points as functions of the input field  $a$  are shown in Fig. 1(b). For a range of  $a$  and  $p$  the map exhibits bistable behavior. As the input amplitude is increased past the point  $a_1$ , the output field jumps to the upper branch at  $U$ . [As the

parameter ranges are broadened, a wide variety of behavior is possible. For example, the graph in Fig. 1(b) can have more than one S bend leading to multiple fixed points. Also for fixed  $a$  and increasing  $p$  or vice versa, period doubling sequences leading to chaotic behavior are observed<sup>4</sup>; but this is not the phenomenon we focus our attention on here.]

Now look at an input field whose transverse profile is Gaussian-like. If  $f \gg 1$ , then the effects of diffraction are initially negligible and at each  $y$  the beam behaves as if it were a uniform plane wave at that amplitude. But, from Fig. 1(b), we see that those points of the Gaussian profile for which  $a(y) > a_1$  will switch up to the upper branch and those parts for which  $a(y) < a_1$  will stay on the lower branch. Therefore at  $x_{\pm}$  where  $a(y_{\pm}) = a_1$  the derivative of the response field is very large. At these locations, diffraction is important and beginning at the edges  $x_+$  and  $x_-$  narrow pulses of width  $\Delta x = O(1/\sqrt{f})$  are generated which eventually fill out the region between  $x_-$  and  $x_+$ , and become the steady-state response of the system. This indeed is the situation observed numerically and shown in Figs. 1(c) and 1(d). What we now show is that these pulses are the solitary waves of Eq. (5). What is particularly new in this study is that the solitary-wave parameters (amplitude and phase) are not determined by initial conditions but by the stable fixed points of the map (6). We develop a theory that predicts their values and our theoretical results are in excellent agreement with the results obtained by numerical experiment. Further, the number of pulses is a function of the transient shape realized after a few passes [Fig. 1(c)] and is proportional to  $\sqrt{f}$  and the maximum input field amplitude.

Taking advantage of the symmetry in  $y$ , the solitary wave of (5) is

$$G_s(y, \zeta) = P(\lambda y, \lambda) \exp[i(\lambda^2 - 1)\zeta/2 + i\gamma], \quad (8)$$

where the shape  $P(\theta, \lambda)$  satisfies ( $\theta = \lambda y$ )

$$P_{\theta\theta} - P + (1/\lambda^2)2P^3/(1+2P^2) = 0. \quad (9)$$

[If we had used a Kerr nonlinearity obtained by taking the small- $P$  limit of (9), the last term in (5) would be  $-G_n + 2G_n^2 G_n^*$  and  $P = \lambda \operatorname{sech}(\theta)$ , the soliton of the nonlinear Schrödinger equation.]

$$G_n(y, 0) = a(y) + RP(\theta, \lambda_{n-1}) \exp[i\gamma_{n-1} + ikL + (i/2)p(\lambda_{n-1}^2 - 1)].$$

Expressing this idea mathematically defines a map  $M$  from  $(\lambda_{n-1}, \gamma_{n-1})$  to  $(\lambda_n, \gamma_n)$ . (The underlying assumption, which is not necessary in the integrable case, is that the change  $\delta\lambda_{n-1}, \delta\gamma_{n-1}$  on each pass is

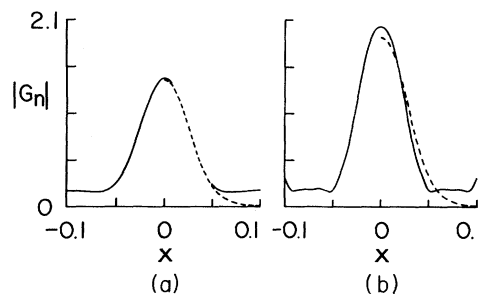


FIG. 2. (a) Comparison of the single-solitary-wave shape ( $N=1$ ) at  $a(0) = 0.1$  predicted from the fixed-point equation (10) (dashed line) with the numerical solution of Eq. (5) (over 200 cavity passes) with boundary condition (6) (solid line). The slight discrepancy in height ( $\sim 1.3\%$ ) may be due to the background radiation evident in the full numerical solution but ignored in the fixed-point equation. (b) The central peak of the seven-solitary-wave train [see Fig. 1(d)] compared to the shape predicted by the fixed-point equation [ $a(0) = 0.194$ ]. The discrepancy in fit ( $\sim 5\%$ ) is consistent with perturbative estimates of changes in shape due to interactions with nearby solitary waves.

We now sketch the basic ideas of our theory. If the equation (5) of profile evolution in the nonlinear medium were indeed the nonlinear Schrödinger equation and therefore integrable, we could decompose  $G_n(y, 0)$  into its soliton and continuous spectrum basis (in which basis the equation is separable) and, using (6), find the soliton and continuous spectrum parameters of the field envelope on the  $n$ th pass in terms of those on the  $(n-1)$ st pass. This would give a representation of the infinite-dimensional map in a separable basis. In most cases, we expect the soliton content of the data to dominate that of the continuous spectrum and therefore the map would naturally reduce to a finite-dimensional one. Further, if the solitons were widely separated [as the solitary wave pulses of  $G$  are in Fig. 1(c)], then to a good approximation, one could obtain a map  $(\lambda_{n-1}, \gamma_{n-1})$  to  $(\lambda_n, \gamma_n)$  for each soliton individually.

Our problem with a saturable nonlinearity is not integrable and we cannot separate the equation in a soliton basis; nevertheless, we can ask what solitary wave  $P(\theta, \lambda_n) e_n^{i\gamma}$  would emerge on the  $n$ th pass from the initial conditions

not too great.) This Letter does not afford us the space to go into the mathematical analysis. This and other details will be given in a longer paper in preparation. The condition that  $M$  has a fixed point  $(\lambda, \gamma)$  can be written

$$\begin{aligned} \sin\gamma \langle \lambda^{-1} P_{\theta} + P_{\lambda}, a(\theta/\lambda) \rangle &= R \sin[kL + \frac{1}{2}p(\lambda^2 - 1)] \langle \lambda^{-1} P_{\theta} + P_{\lambda}, P \rangle, \\ \cos\gamma \langle P, a(\theta/\lambda) \rangle &= \{1 - R \cos[kL + \frac{1}{2}p(\lambda^2 - 1)]\} \langle P, P \rangle. \end{aligned} \quad (10)$$

In (10),  $\langle P, Q \rangle = \int_{-\infty}^{\infty} P(\theta) Q(\theta) d\theta$ . This is the principal analytic result of the Letter. We solve (10) numerically for a number of cases with different parameter values and compare our predicted solitary-wave shapes and amplitudes with those obtained by numerical experiment. These results are summarized in Figs. 2(a) and 2(b).

We emphasize that these solitary waves, which are the transverse nonlinear normal modes of the cavity, are the infinite-dimensional analogs of the upper-branch plane-wave fixed points given in Fig. 1(b). By analogy with that case and the low-Fresnel-number results of Ref. 5, we expect that, as the parameter ranges are broadened, a rich variety of behavior will occur. This should include period doubling and other routes to states of temporal chaos in which the solitary wave amplitudes flutter chaotically but in which states an overall spatial coherence is maintained.

We thank the U. S. Army Research Office, the U. S. Air Force Office for Scientific Research, and the National Science Foundation for support

of these studies.

<sup>1</sup>See A. J. Lichtenberg and M. A. Leiberman, *Regular and Stochastic Motion* (Springer, Berlin, 1983), p. 446.

<sup>2</sup>A. R. Bishop, K. Fessler, P. S. Lomdahl, W. C. Kerr, M. B. Williams, and S. E. Trullinger, *Phys. Rev. Lett.* **50**, 1095 (1983); J. C. Eilbeck, P. S. Lomdahl, and A. C. Newell, *Phys. Lett.* **87A**, 1 (1981).

<sup>3</sup>J. V. Moloney and H. M. Gibbs, *Phys. Rev. Lett.* **48**, 1607 (1982).

<sup>4</sup>An enormous literature exists on optical bistability and associated instabilities. A comprehensive review of the subject may be found in *Optical Bistability*, edited by C. M. Bowden, M. Ciftan, and H. R. Robl (Plenum, New York, 1981). The first prediction of chaos in a ring cavity was by K. Ikeda, *Opt. Commun.* **30**, 257 (1979) [see also K. Ikeda, H. Daido, and A. Aki-moto, *Phys. Rev. Lett.* **45**, 709 (1980)].

<sup>5</sup>J. V. Moloney, F. A. Hopf, and H. M. Gibbs, *Phys. Rev. A* **25**, 3442 (1982). This work predicts that the transverse profile will undergo transitions to chaos via periodic, quasiperiodic, and frequency locking when the Fresnel number is small.